PROCEEDINGS, 51st Workshop on Geothermal Reservoir Engineering
Stanford University, Stanford, California, February 9-11, 2026
SGP-TR-230

Extending Permeable Fracture Imaging at Newberry to Depth: Added Receiver-Coverage Area and Seismic Velocity Control.

Jeffrey Eppink, Peter Malin, Tom Fleure, Frank Horowitz, Austin Mathews, Bill McLain, Hector Ontiveros, Charles Sicking, Anastasia Stroujkova, Jan Vermilye, Sergio Valenzuela, Tingjun Chen, Zehao Wang, and Alain Bonneville

Enegis LLC, 10300 Eaton Place, Fairfax, VA 22030

jeppink@enegis.com

Keywords: Passive seismic method, emissions from fluid-filled fractures, velocity data collection, signal processing, PFI results

ABSTRACT

In September 2025 we conducted a 3-week, 1,323 seismic receiver, Permeable Fracture Imaging (PFI™), survey at Newberry Volcano. The survey was aimed at extending a previous, 2023, 982 receiver, PFI survey from ~2.2 km to over 3 km. The extension included adding (1) more receivers to cover a broader area (and hence adding depth) and (2) refining the seismic velocity-depth profile using surface vibroseis, behind casing distributed acoustic sensing (DAS), and a downhole propellant-burn sourced check shot (hence adding absolute travel time resolution). We received support for both the 2023 and 2025 surveys from the Advance Research Project Agency – Energy (ARPA-E), and in 2025, from our industrial partner, Mazama Energy. Geothermal Energy Research and Development, Ltd, provided support for the DAS operation. Additionally support in 2023 came from Quaise Energy.

The PFI method uses hundreds of time-synced seismic recorders to observe episodes of small seismic movements in connected permeability structures – the fluid filled joints, fractures, fracture zones, faults, and fault zone that are geothermal drilling targets. The signals are enhanced by stacking time-distance adjusted seismic signals for a subsurface volume of voxels. The voxel size depends on the density of receivers – spread at roughly 36 receivers per km^2 in both surveys. The depth penetration of PFI depends on uniform coverage over the target area plus a buffer area, the width of which needs to be greater than 1 x the depth of the target. In 2023 the area was 27 km^2 , yielding a PFI depth of 2.2 km. In 2025, by adding 338 receivers at the same density, the area increased to 37 km^2 and PFI depth to more than 3 km. In both cases, the resulting resolution was voxels roughly 30x30x30 m in dimension.

The spatial accuracy of the PFI method depends on an accurate 3D seismic velocity model. This includes the need to know the varying thicknesses and velocities of near-surface sediments (such adjustments are known in O&G seismic reflection methods as "static corrections") and the velocity profile all the way down to the bottom of the PFI target. To address this requirement, in the 2025 survey we employed (1) 3-D vibroseis-source profiling recorded into the 1,323-receiver surface net, (2) a 2,736 m long, cemented behind casing, DAS cable and (3) a propellant-burn check-shot at ~ 3000 m depth. The vibroseis-to-surface net covered the upper velocity structure. The propellant check shot recorded on the DAS covered the mid and deeper structure.

The processing of the resulting terabyte volume of passive PFI data was significantly hampered by the continuous surface operation of injection pumps at the head of the 55-29 well. Using the available 8 hours of quiet-time hours of data when the pumps were turned off, we were able to image a zone of high-angle west dipping features below the depth of the 2023 survey. In map view, these features show the same NW and conjugate NE trends as in the 2023 data. One important high-PFI-amplitude zone in the NE corner of our 2023 target area appears to extend further depth in the 2025 data. Using special PFI processing, we identified high-amplitude PFI signals coming from near-well features along ~3000 m deep perforated zone of 55-29. These turned out to be from the Stimulated Reservoir Volume (SRV) between this injection well, the 55-29 producer well, and the surrounding volume – the latter suggesting connection to a much larger SRV. Moreover, it appears that the propellant-burn check-shot also stimulated PFI signals from around 55-29, including a ~300 m long channel extending southwest from well 55-29.

1. INTRODUCTION

The PFI™ method maps the locations of permeable fractures using ambient seismic recording. It is important to note that PFI does not use microearthquakes as a mapping tool. Instead, PFI maps the locations of fluid filled fracture that connect to form the permeability field. Such fractures have been found to emit seismic tremors, which are then passively mapped with either a temporary surface or permanent borehole network of seismic receivers (e.g. Sicking and Malin, 2019).

Our 2023 Newberry survey was designed to locate fluid-filled fractures extending from the Newberry Geothermal Field's 3 km deep Well 55-29. Early in 2023 we modeled the location and resolution tradeoffs for several distributions of seismic velocity, PFI signal depths, recorder spacings, and network size. Based on them, we deployed 982 can-sized seismic recorders, nominally 175 m apart, over a 27 km2 area west of Lake Paulina (e.g. Fig 1; from Eppink et al., 2025). This network captured PFI signals above a ~2.2 km deep, ~2.75 km2 patch centered on the 3 km deep 55-29 well (Fig 2; ibid; please refer to this paper for a more complete background).

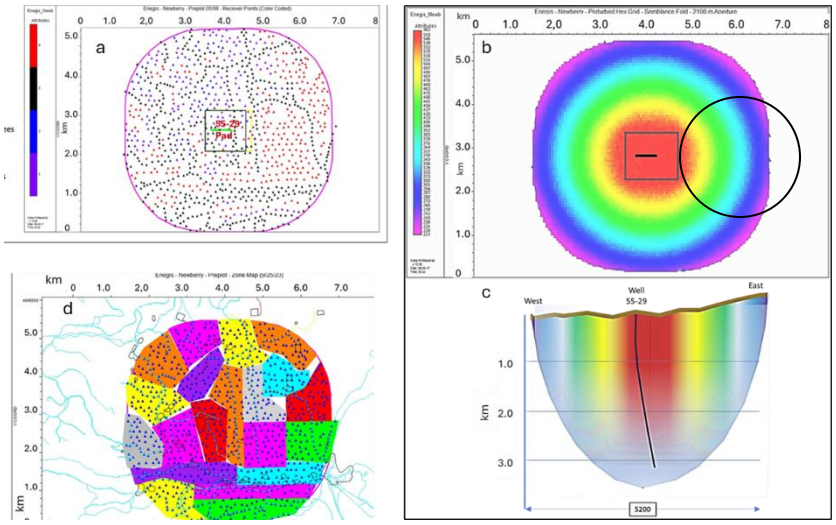

Figure 1. (a) The 2023 PFI network footprint and station locations adjusted to road access for time-efficient deployment. (b) A color code map of stacking fold. The black circle –called the aperture - illustrates how the number of stations within it, all of which are used to make the stack, falls off as it approaches the network's edges. The stacking fold ranges from red > 575 to purple > 225. (c) the depth/resolution ellipsoid associated with the signal processing aperture as the number of receivers inside of it falls off toward the edges. (d) a logistics division of the network into ~50 station-containing blocks for deployment.

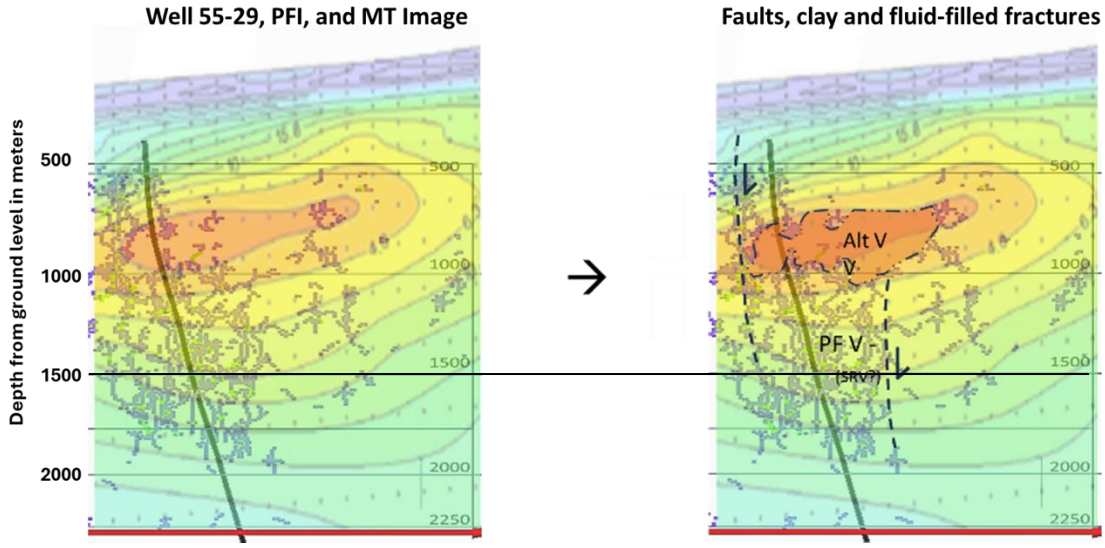

Figure 2. (a) An EW vertical cross section through the 2023 cloud of PFI activity around Well 55-29, displayed using the traces of local PFI signal maxima. These are the *tracks* of connected voxels within the PFI cloud, interpreted as showing the centers of permeability channels. (b) The PFI map interpreted in terms of normal faults and the low permeability clay cap observed in the resistivity data. The marker line at 1500 m depth corresponds to the one shown in Figure 3.

2. THE OBJECTIVES OF THE 2026 PFI SURVEY.

In September 2025 we conducted a 3-week, 1,323 seismic ground-level receiver, PFI field campaign at Newberry. The broad objective was to extend the previous 2023 PFI survey from ~2.2 km to over 3 km depth. The spatial accuracy of the PFI method depends on an accurate 3D seismic velocity model. This includes near-surface adjustments known in reflection seismic methods as “static corrections” and the velocity profile down to the PFI target, in this case the 55-29-to-55A-29 well-doublet connection. To address this requirement, in the 2025 survey we employed 3-D vibroseis-source signal recorded into the 1,323-receiver surface net, a 2,736 m long, cemented behind casing, DAS cable, and a propellant-burn velocity check-shot at 2989 m depth. At the same time, a propellant burn can work also as a hydroshear-like permeability stimulation with fewer inducted earthquakes.

The specific Objectives of the 2025 survey included: 1. Map PFI signals coming from below the 2023 survey and past the depth of the 55-29 / 55A-29 doublet. 2. Imagine the SRV connections between wells 55-29 and 55A-29 at 3 km. 3. Measure near-surface velocity

static-corrections in volcanic terrains using vibroseis sources. 4. Utilizing the DAS cable in well 55-29 for deep velocity studies. 5. Use a perforated-casing safe downhole-propellant-burn for velocity calibration and permeability stimulation – the latter also tested for reduced induced seismicity.

To meet Objective (1) the survey extensions included adding more receivers to cover a broader area, hence adding depth. Prior to our 2025 survey, Well 55-29 was stimulated with proprietary permeability enhancement methods. Thus, Objective (2) sought to map the resulting connections between Well 55-29 and 55A-29. Objective s (1) and (2) required refining the deep velocity structure below, which we addressed by: (3) near-offset vibroseis signals; (4) behind casing distributed acoustic sensing (DAS), and (5) a well-bottom propellant-sourced deflagration burn, which has been shown to avoid potential perforated casing damage.

The strain rate of a propellant deflagration burn is orders of magnitude slower than a detonation, but proportionately faster than hydraulic stimulation. As a result, this stimulation method has been shown in mine tests followed by back-excavation measurements of induced-fractures, to produce permeable channels longer than high energy detonations and shorter than high pressure fluid fracks. With respect to the latter characteristic, a propellant deflagration is more like a hydroshear stimulation, opening pre-existing permeable fractures whose shorter lengths are less likely to produce noticeable earthquakes.

3. RESULTS

The prime objective of the 2025 survey was to obtain a PFI image around below and congruent with both the 2023 survey and the known geology, and geophysical and well observations. For the reasons noise related to the pump noise, the usable 2025 PFI data and their interpretation begins with the lower half of the 2023 results, the top of which coincides with the top of the 2025 PFI (Figure 3).

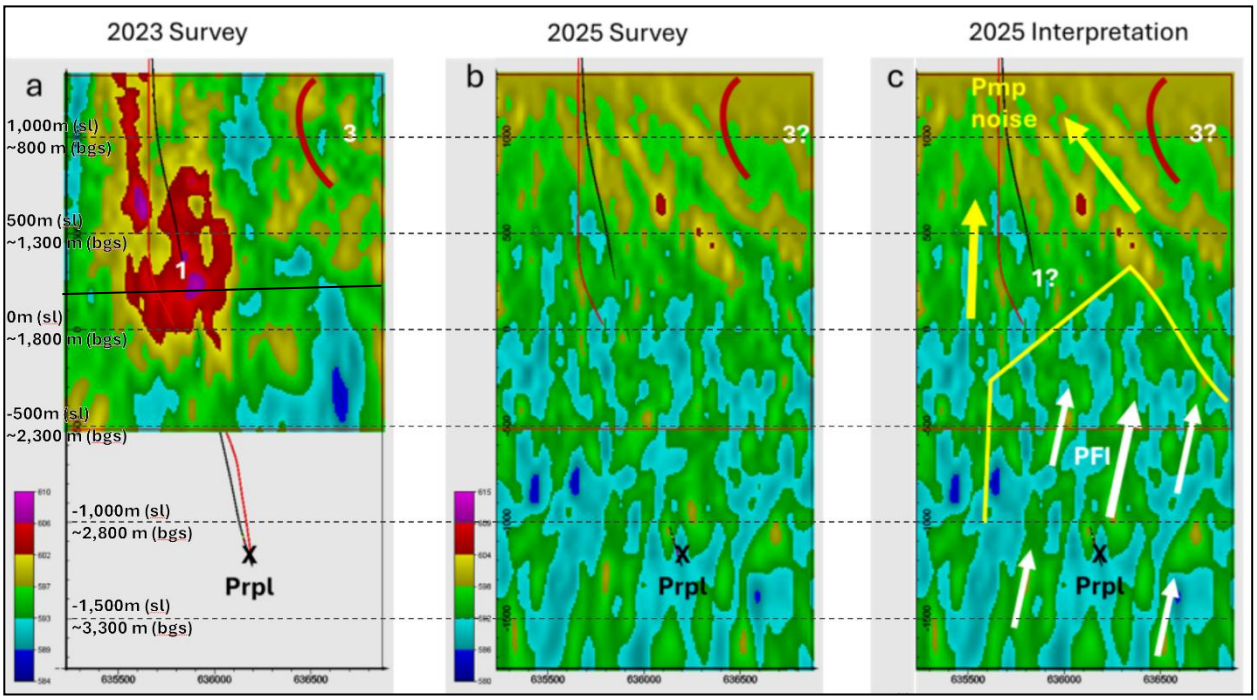

Figure 3. EW vertical slices through the 3-D volumes at the 55-29 well toe location for the lower half of the 2023 and 2025 survey. The propellant burn velocity calibration location is at the x labeled Prpl. The view is from the south. Well 55-29 is the black line and well 55A-29 is the red line. The black marker line in a. is at the same level as in Figure 2. b. Shows the same slice in 2025. The area of a 2023 high activity feature labeled 3, shown by circular line, has been projected on to this slice for further reference. b. & c. The pumping noise is expressed as sloping energy highs pointing toward the surface well pad location in the shallow portion of the 2025 volume. As indicated in c., we interpret the loss of far-offset feature 1 as due to this noise swapping the PFI signal. The cone of this noise is indicated by the yellow lines and arrows. Below these lines we suggest there is a zone of well resolved PFI signals. These are seen in the horizontal slices in Figure 4, which are congruent with the 2023 result and regional geology and geophysics.

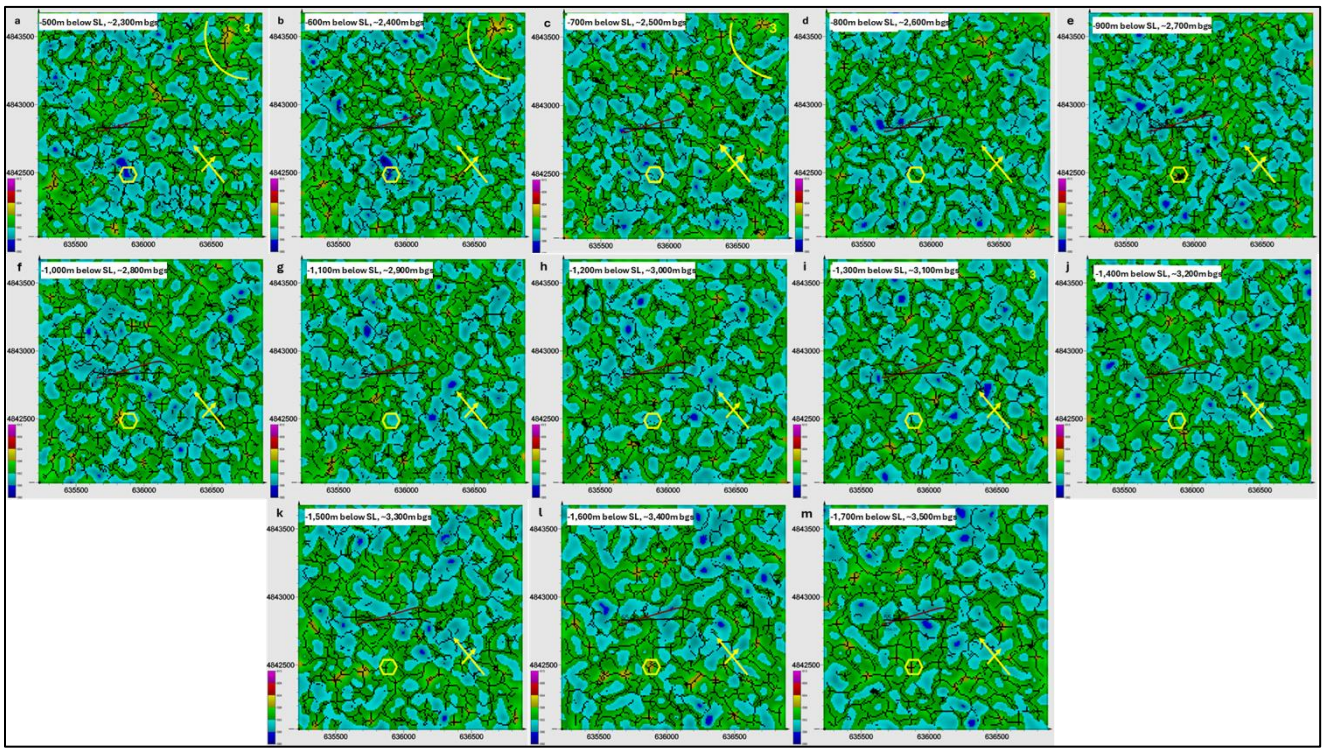

Figure 4. Depth slices through the 2025 survey volume as viewed from above. The depth is shown on the upper left and a structural orientation arrow from the regional geology is shown in the SE. The fixed size hexagons in each plot help reveal the decreasing density of PFI signals with depth, interpreted as result of the closing of fracture. The locations of the 55-29 and 55A-29 wells are shown in black and red lines for reference, but these wells do not extend below 1200 m BSL - slice h. Slice c is shown in a display scheme to bring out the high density of short PFI features. The map area of feature 3 is shown on the first three depth slices (a, b, c), below which it no longer appears to be present. The constant size hexagonal also highlights the SE area where several high amplitude PFI features appear in depth slices l, m, and n.

Given that the lease operator was actively conducting injection and flow tests into a pair of wells, we were able to image the flow between the wells using PFI (Figures 5, 6, and 7). The in-line distance between the perforated liners of the two wells is ~125 m. This bottom ~250 m interval was previously stimulated by the operator using proprietary industry permeability enhancement tools. It is where we also conducted our propellant-burn seismic velocity calibration shot. As shown in our 2023 Low Pressure stimulation study, strong PFI signals can be generated by low-level fluid flows in connected fractures. This also proved to be the case in our 2025 survey during the many overlapping days the reservoir development pumps were in operation. Near-wellbore PFI imaging requires a very accurate velocity model, so the PFI signals can be correctly placed with respect to the perforated zones. Since the propellant burn was done in the toe of Well 55-29 and the travel time from there to the ground array was well known, we were able to meet this requirement. The results for well-to-well flow over an 8-day period are shown in Figures 5 and 6.

4. CONCLUSIONS

The specific Objectives of the 2025 survey described in Section 2 were by-and-large met. The velocity model obtained from the static correction survey and the combination of the 55-29 Well DAS cable and propellant burn allowed us to accurately place PFI features in the target volume below the 2023 survey depth. The resulting cross sections and horizontal map slices revealed a deep zone of west dipping, NW trending, high angle features congruent with the 2023 survey and local geology. When processed using high amplitude signals from the perf zones of the 55-29 / 55A-29 wells, the PFI data mapped both interpreted fluid-flows in the gap between these wells and connections to potential natural permeability zones offset from it. We believe this is an important result for long-term stability of the advected heat flowing into the 55-29 production well. While the PFI method of collecting and processing ambient signals does not make use of microearthquake events, they can still be found in these data, particularly during stimulation procedures, check-shots and production pumping. A search for earthquake events in spectrograms of our unprocessed PFI data did not reveal a cloud of such events.

Two important lessons from the 2025 survey are: 1) the critical need to record far-offset PFI data during quiet times, and 2) the high-energy of near well hydraulic flow can overcome even otherwise very problematic pump noise.

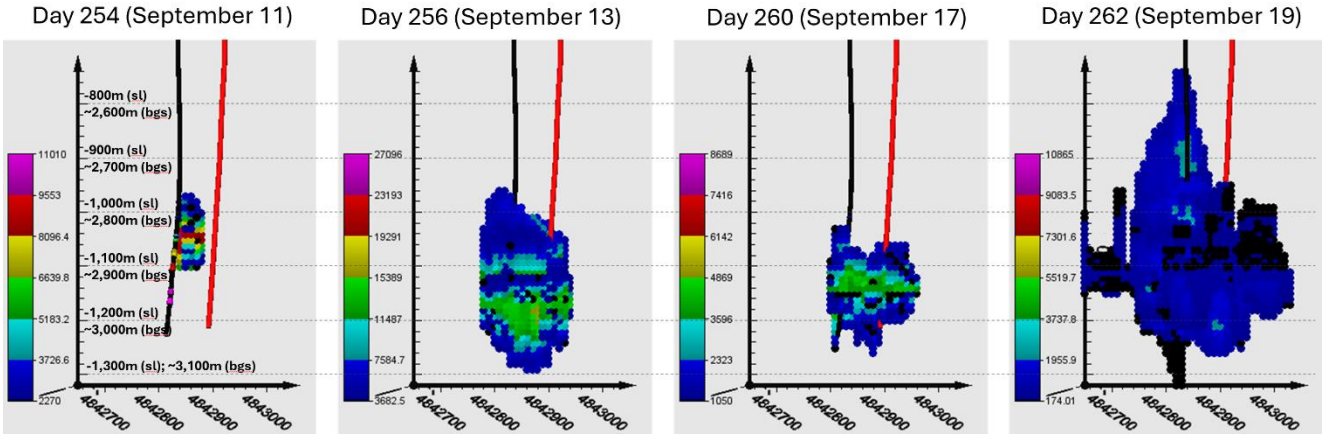

Figure 5. Near-well PFI images can be obtained from time windows containing high energy signals from the perforated section. The time sequence plots of this activity surrounding the 55-29 / 55A-29 doublet are shown as seen from the east. Each plot shows a projection of the volume of high PFI activity. The differences between plots are interpreted as reflecting the opening of different natural channels, which extend beyond the well-to-well connections.

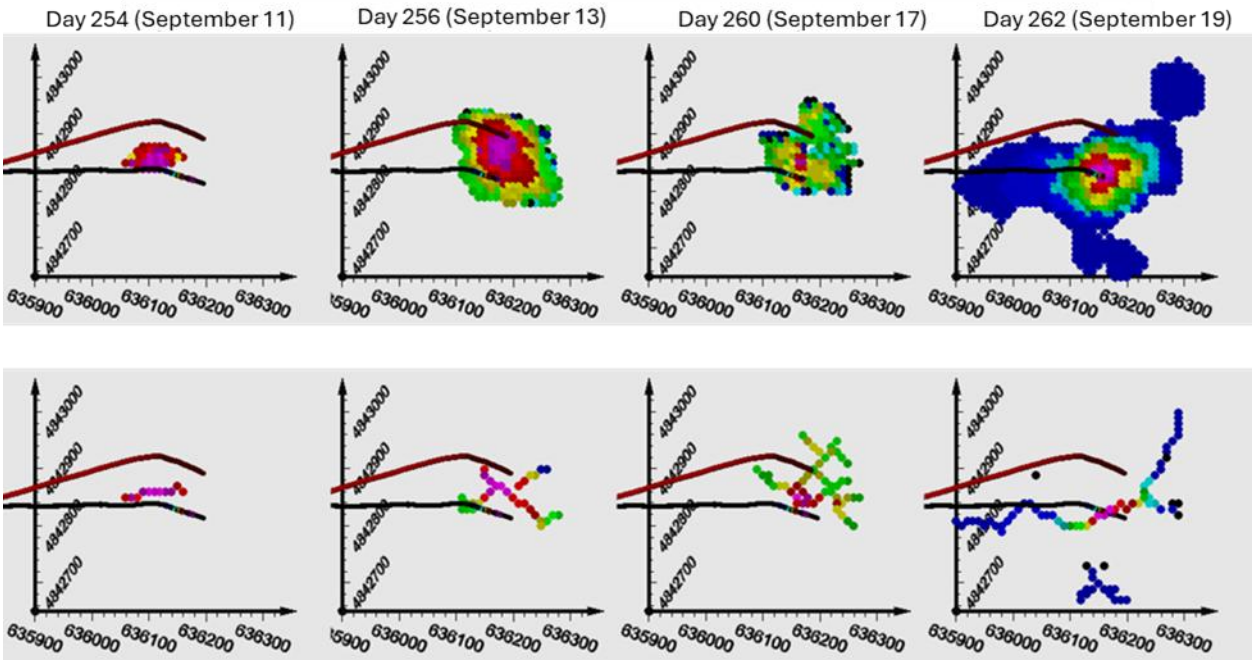

Figure 6. The top row of this image shows a map slice through the maximum PFI activity in Figure 5. The lower plots show the connected traces of voxels with the highest PFI activity. Combined with Figure 5, these images show the stimulated reservoir volume extends to the north and west below the gap between 55-29 and 55A-29. We interpret these results as showing the opening of natural fractures surrounding and connecting to the two wells.

REFERENCES.

Eppink, J., Fleure, T., Malin, P., Mathews, A., McLain, W., Sicking, C., and Stroujkova, A.: Drilling Target Mapping at Newberry with Passive Seismic Permeable Fracture Imaging (PFI), PROCEEDINGS, 50th Workshop on Geothermal Reservoir Engineering, Stanford University, Stanford, CA (2025).

Sicking, S. and Malin, P.: Fracture Seismic: Mapping Subsurface Connectivity. *Geosciences* **2019**, *9*, 508. https://doi.org/10.3390/geosciences9120508 (2019)